Available online at www.sciencedirect.com

SciVerse ScienceDirect

www.elsevier.com/locate/matchar

Hydrogen-induced toughness drop in weld coarse-grained heat-affected zones of linepipe steel

Jung-A Lee[a], *Dong-Hyun Lee*[a], *Moo-Young Seok*[a], *Un Bong Baek*[b], *Yun-Hee Lee*[b], *Seung Hoon Nahm*[b], *Jae-il Jang*[a,*]

[a]*Division of Materials Science & Engineering, Hanyang University, Seoul 133-791, South Korea*
[b]*Division of Industrial Metrology, Korea Research Institute of Standards and Science, Daejeon 305-340, South Korea*

ARTICLE DATA

Article history:
Received 2 April 2013
Received in revised form 28 April 2013
Accepted 4 May 2013

Keywords:
Steel
Hydrogen
Toughness
Heat-affected zone

ABSTRACT

In this study, hydrogen effects on the impact toughness of simulated coarse-grained heat-affected zones (CGHAZs) in a linepipe steel were investigated in search of the possible "local brittle zone phenomenon" in hydrogen pipeline welds. After hydrogen charging, the inter-critically reheated and unaltered CGHAZ exhibited very low impact energies as well as occurrence of splitting. This hydrogen-induced toughness drop is discussed in terms of combined effects of brittle microstructures and hydrogen trapping.

1. Introduction

In the context of this century's major energy-related issues arising from the non-renewable nature of fossil fuels and serious air pollution, recent interest in the use of hydrogen as an alternative main energy source has increased explosively. For preparing the up-coming era of the so-called "hydrogen economy," development of hydrogen infrastructures is essential. Particularly, hydrogen delivery is a critical issue for the widespread use of hydrogen. It has been reported that, among various transportation methods, a pipeline network infrastructure may be the most cost-effective and energy-efficient way to transport large amounts of hydrogen over long distance [1,2]. However, new design and construction of hydrogen pipelines may require high initial capital costs. A low-cost option for partly overcoming this issue is transporting gaseous hydrogen (in a form of either pure hydrogen or a blend of natural gas and hydrogen) using the existing natural gas pipelines [1,2].

One of the major concerns arising from hydrogen transportation through the existing natural gas pipelines under very high pressure level (up to ~3000 psi or ~21 MPa) is the influences of hydrogen entry and permeation on the mechanical performance of the pipeline steels. It is widely accepted that hydrogen almost always deteriorates the mechanical properties of materials by various ways including hydrogen embrittlement (HE), hydrogen-induced cracking (HIC), hydrogen attack (HA), sulfide stress cracking (SSC), and stress corrosion cracking (SCC) [3]. These hydrogen effects can be also available for the natural gas pipeline steels (that are specified by the American Petroleum Institute, API). Aside from the hydrogen pipeline issue, the influence of hydrogen in API steels has been studied for different purposes such as assessment of API steels' resistance to sour environment [4,5].

An important issue remaining unsolved yet may be the influence of hydrogen in weld heat affected-zones (HAZs) of the pipeline steels. The hydrogen effects in base metal may

* *Corresponding author.*
E-mail address: jijang@hanyang.ac.kr (J. Jang).

1044-5803/$ – see front matter © 2013 Elsevier Inc. All rights reserved.
http://dx.doi.org/10.1016/j.matchar.2013.05.001

be very different from that in HAZ since welding can seriously alter (and generally degrade) the metallurgical and thus mechanical properties of materials. Especially, the coarse-grained HAZs (CGHAZs) adjacent to the weld fusion line often exhibit abnormally low fracture resistance and thus are referred to as local brittle zones (LBZs) in multi-pass welded joints [6–9]. Thus, analysis of the hydrogen effects in the CGHAZs may be essential for ensuring the safety and long-term reliability of the hydrogen transmission pipeline infrastructure. Nevertheless, somewhat surprisingly, little systematic research on the issue (i.e., hydrogen effects in CGHAZs) is available in the literature. As the first step to shed light on the issue, here we systematically explore (for the first time, to the best of our knowledge) the hydrogen effects on the toughness of pipeline steel CGHAZs to find out the possible LBZ phenomenon in hydrogen pipelines.

2. Experimental

The material examined in this study was a commercial grade API X70 steel, one of the most popular natural gas pipeline steel, whose chemical composition is 0.07C–0.25Si–1.55Mn–0.25Cu–0.2Ni–0.03V–0.015Ti–0.04Nb–0.03Al and balanced Fe (wt.%).

For systematic and reproducible evaluation of the local properties in HAZ, HAZ simulations were performed with a Gleeble 1500 thermo-mechanical simulator (DSI, Poestenkill, NY). The thermal cycles for HAZ simulation are typically characterized by both the peak temperature (T_P) and cooling time from 800 to 500 °C ($\Delta t_{8/5}$) which represent distance from heat source and welding condition, respectively. After reaching the first peak temperature (T_{P1}) of 1350 °C, the specimens were cooled down for a given $\Delta t_{8/5}$. Subsequently, the specimens were reheated to the second peak temperature (T_{P2}), and then cooled down under the same rate. Through a modified equation based on Rosenthal's heat flow formula [10], the $\Delta t_{8/5}$ was calculated as 18 s that is approximately equivalent to the cooling rate of a shielded metal arc welding (SMAW) of 17-mm-thick plate with a heat input of 30 kJ/cm. Microstructures of both base metal (BM) and simulated HAZ specimens were observed with an optical microscopy (CK40M, Olympus, Tokyo, Japan) using samples whose surfaces were mechanically-polished and then etched with 3% nital. To identify the strength variation within the CGHAZs, Vickers hardness tests were performed at maximum load of 9.8 N with HMV-2 equipment (Shimadzu, Tokyo, Japan).

Electrochemical hydrogen charging was performed on a potentiostat (HA-151A, Hokuto Denko, Tokyo, Japan) using a 0.25 g/L As_2O_3 in a 1 N H_2SO_4 solution. The As_2O_3 was added for enhancing the hydrogen atom permeation and avoiding their recombination. While platinum and the specimen were used as anode and cathode respectively, hydrogen was charged into specimens at an electrochemical current density of 100 mA/cm^2 for 24 h at room temperature (RT).

Standard Charpy V-notch impact tests were performed on both hydrogen (H)-free and H-charged samples at RT and −40 °C using a 500 J-capacity tester (CI-500D, TTM, Tokyo, Japan). The H-charged samples were tested within 20 min after charging. Fracture surfaces were observed through a scanning electron microscopy (SEM, JCM 5700, JEOL Ltd, Tokyo, Japan).

3. Results and Discussion

Generally, the CGHAZs are roughly subdivided into four characteristic zones according to the peak temperature of subsequent thermal cycles in a multi-pass welding procedure [7,8]; (1) the unaltered (UA) CGHAZ, the region reheated above the specific temperature of grain growth or not reheated at all, (2) the super-critically reheated (SCR) CGHAZ, the region reheated to the temperature just above A_{C3}, (3) the inter-critically reheated (IC) CGHAZ, the region reheated to austenite/ferrite two phase region ($A_{C1} < T_{P2} < A_{C3}$), and (4) the sub-critically reheated (SC) CGHAZ, the region for $T_{P2} < A_{C1}$. Among them, the SCR CGHAZ is often treated as fine-grained HAZ (FGHAZ) due to its recrystallized fine grains. The present study was focused on the UA, SCR, and IC CGHAZ. The SC CGHAZ is not considered here because its properties are expected to be similar (or a little superior) to the UA CGHAZ due to its low peak temperature and tempering effects [8]. For the HAZ simulations, the A_{C1} and A_{C3} were determined as ~713 and ~860 °C, respectively, based on Andrews' empirical formula [11]. Thus, in this study, the T_{P2} was taken as 1350, 1050, and 800 °C for the UA, SCR, and IC CGHAZ, respectively.

Vickers hardness values and representative microstructures of three simulated CGHAZs are presented in Fig. 1. While microstructure of BM mainly consists of ferrites with very small fraction of pearlite (not shown here), both the UA and IC CGHAZ exhibit bainitic laths within coarsened prior austenite grain. The SCR CGHAZ has very fine matrix (and thus often called FGHAZ, as mentioned before) since its second thermal cycle above A_{C3} induced grain refinement by recrystallization. Although the UA and IC CGHAZ have coarsened structure, they show higher hardness than the SCR CGHAZ and BM, which may be due to their bainitic structure having very high matrix strength.

Fig. 2a summarizes the room-temperature Charpy impact test results of both the H-free and H-charged CGHAZs as a function of T_{P2}. Before hydrogen charging, the SCR CGHAZ shows the highest impact energy (~429 ± 30 J) that is even higher than that of the BM (~400 ± 40 J). In contrast, the H-free UA and IC CGHAZ exhibit much lower average impact energy with a larger scatter (~83 ± 51 J and ~ 106 ± 65 J, respectively)

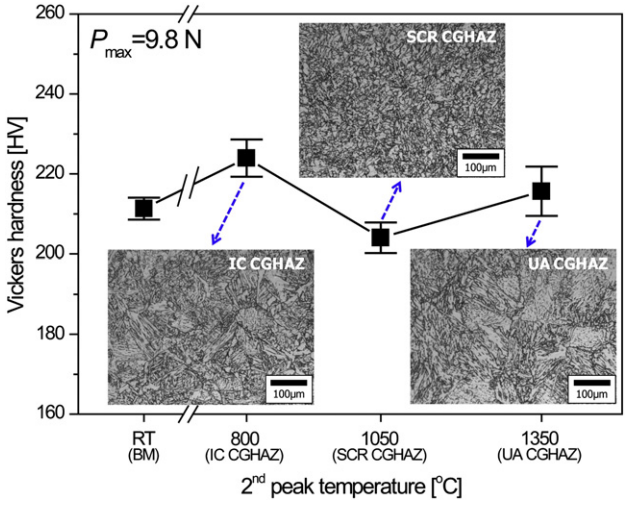

Fig. 1 – Microstructures and hardness of the three simulated CGHAZs.

than that for the SCR CGHAZ and BM. Hydrogen charging resulted in dramatic loss in toughness; after charging, the impact energies of all CGHAZs were lower than that of the BM (~219 ± 44 J). Especially, the UA and IC CGHAZ show very low impact energies (~31 ± 9 J and ~26 ± 7 J, respectively), while the SCR CGHAZ has still not-too-low toughness (~88 ± 5 J). It is noteworthy that, according to the pipeline steel specification of API 5 L for the 16–20 mm-thickness pipelines, the required minimum impact energy at 0 °C is 27 J [12]. Fig. 2b shows the results from impact tests at −40 °C. Since the trend of toughness variation at this temperature is similar to that obtained at RT, only one test for each condition was performed for the sake of simplicity. It is noteworthy that, in both H-free and H-charged samples, the IC CGHAZ shows obvious decrease in impact energy with varying temperature from RT to −40 °C and has very low toughness at −40 °C (~8 J for H-free sample and ~3 J for H-charged one), whereas toughness of the UA CGHAZ is almost unchanged at RT and −40 °C. This implies that, RT is already in the lower shelf energy regime for the UA CGHAZ, but is still in the ductile-to-brittle transition regime for the IC CGHAZ, suggesting that the IC CGHAZ may be the most brittle among the three CGHAZs.

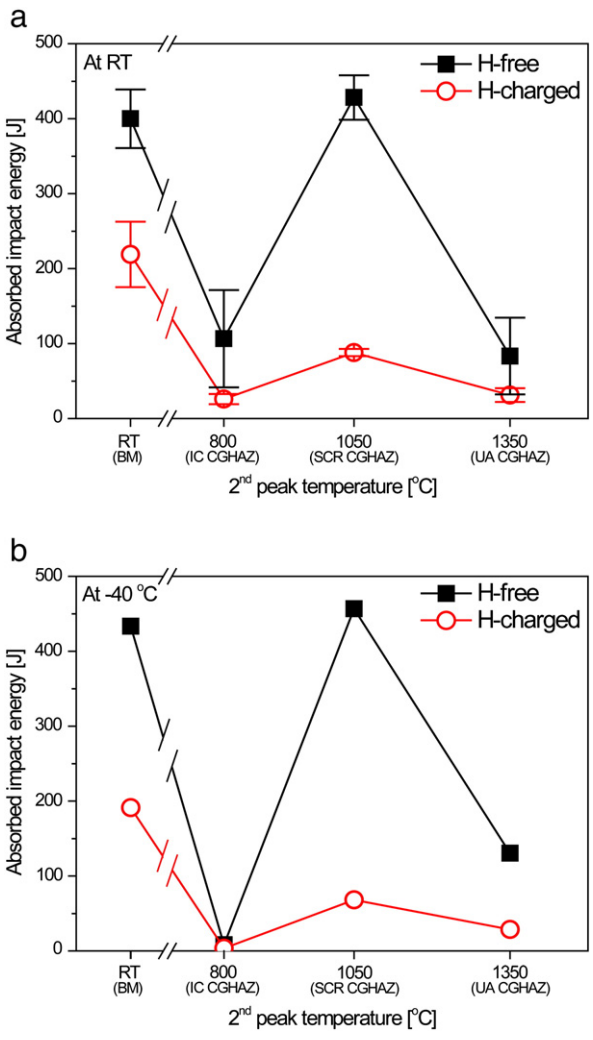

Fig. 2 – Variations in Charpy absorbed energy of the simulated CGHAZs obtained at (a) RT and (b) −40 °C.

Representative fractographs of the samples tested at RT are presented in Fig. 3. For the SCR CGHAZ, the H-free samples show the dimples for ductile rupture whereas the H-charged samples exhibit the mixed feature of ductile dimples and small portion of localized quasi-cleavage fracture. As can be expected from large toughness fluctuations in Fig. 2a, the H-free UA and IC CGHAZ show a variety of fractographic appearance; i.e., while some samples with relatively high impact energy indicate ductile fractographs (not shown here), other samples with low energy show clear evidence for brittle cleavage fracture (e.g., see Fig. 3a and e, of which energies were ~47 and ~61 J for the UA and IC CGHAZ, respectively). In the H-charged UA and IC CGHAZ, fracture surfaces clearly indicate the occurrence of brittle cleavage fracture. Inset images of Fig. 3 provide the macroscopic view of the fractured surfaces, which is in consistent with the SEM fractographs; shear lips (that is, an evidence for ductile fracture) are observed only in the SCR SGHAZ and are absent in the UA and IC CGHAZ. Very interestingly, for the UA and IC CGHAZ, one can find a clear difference in the macro-views between H-charged and H-free samples; that is, only in the H-charged samples, one (or two) relatively large crack(s) was reproducibly observed across the brittle fracture surface. Since the presence of this crack (so-called "splitting," "separation," "delamination") is the main difference between the H-free and H-charged specimens, it seems closely related to the hydrogen-induced loss in toughness. Examining the faces of the splitting revealed that the cracking occurred in a brittle manner, as shown in Fig. 3g.

All above results propose that the IC and UA CGHAZ are the strong candidates for the primary and secondary LBZs of hydrogen pipeline steel welds. Since the LBZ behavior at RT was observed only in the H-charged samples, one may call the embrittlement as "hydrogen-induced LBZ phenomenon." This LBZ phenomenon is undoubtedly attributed to the combined effects of weak microstructure and hydrogen embrittlement.

Relatively low toughness of the H-free IC and UA CGHAZ can be explained by coarsened microstructure and martensite–austenite (M–A) constituents (or sometimes called "martensite islands"). Although there is some controversy on the detailed role of the M–A constituents, it is well accepted that the M–A constituents lead an environment to assist brittle fracture of themselves or neighboring matrix. Therefore, the first step of the LBZ analysis was observation of the M–A constituents with SEM using the samples especially prepared by a two-stage electrolytic etching [13]. Fig. 4 provides typical SEM images of the M–A constituents. In the figure, the white phases are M–A constituents remaining after the two-stage etching, which is supported by their very high carbon contents shown in the map of electron probe micro-analysis (EPMA) in Fig. 4a. Fig. 4b and 4c indicate that both the UA and IC CGHAZ have a large amount of M–A constituents. The geometry of M–A constituents could be divided into two categories; a stringer type M–A between along bainitic lath boundaries and a blocky type M–A at the prior austenite grain boundaries. While the stringer type M–A constituents are known to crack readily, the cracking of the blocky type M–A constituents is rarely reported [7]. Note that, in this study, the blocky type M–A constituents were observed only in the IC CGHAZ (Fig. 4c) and were not found in UA CGHAZ (Fig. 4b). The reason for this difference is not clear at this point, which needs further investigation. Area fraction of M–A constituents in IC

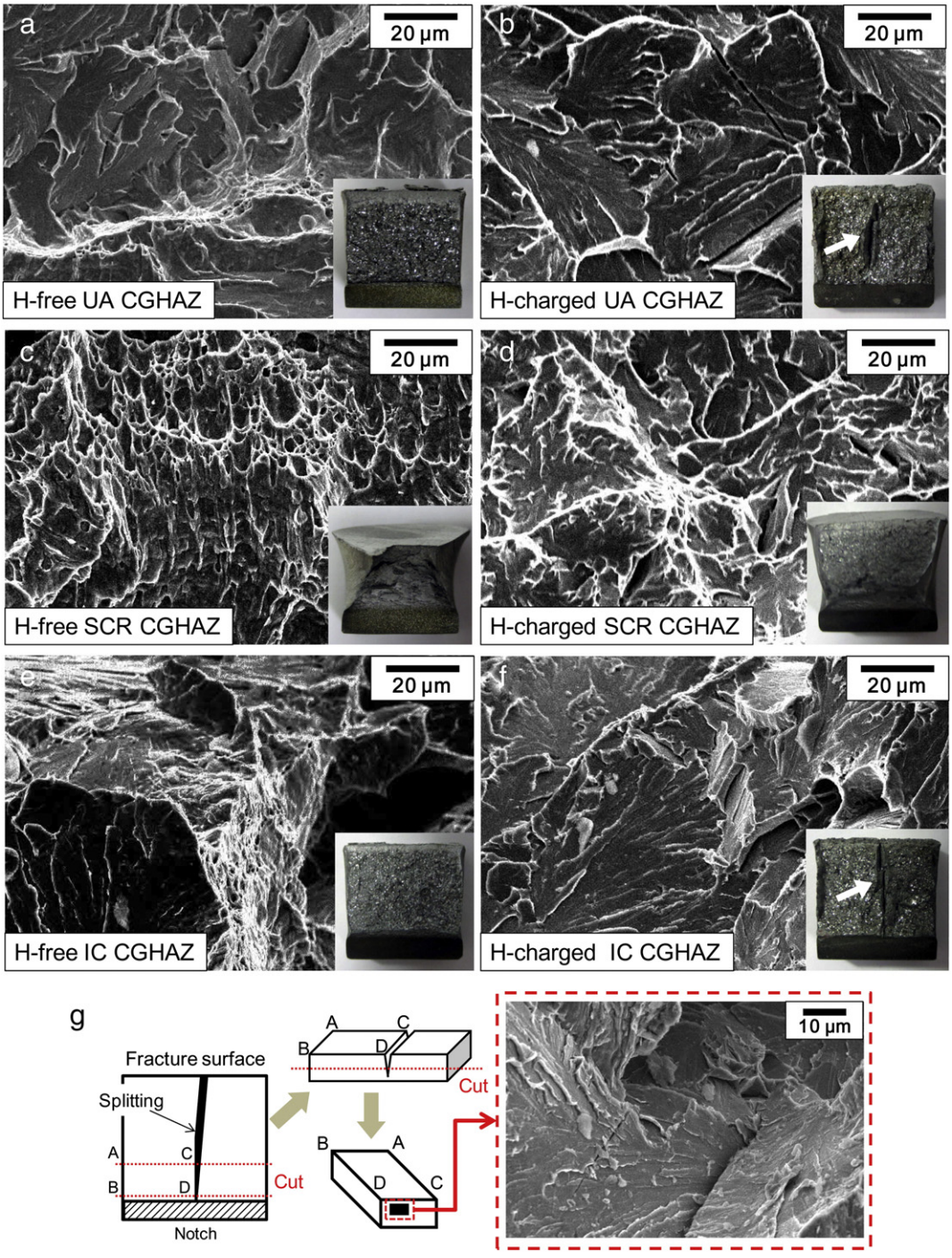

Fig. 3 – Fracture surfaces of the three CGHAZ samples tested at RT: (a), (c), and (e) are for H-free samples, and (b), (d), and (f) are for H-charged samples. In (b) and (f), splitting is indicated by white arrows. The surface of the splitting is provided in (g) with schematic illustration of cutting procedure.

CGHAZ (~17.8%) was more than twice of that in UA CGHAZ (~8.6%). However, it has been suggested that, in addition to the fraction and type (i.e., blocky or stringer) of M–A constituents, the carbon contents of M–A constituents can also be a parameter affecting toughness [9]. The existence of M–A constituents may also explain high hardness of the H-free IC and UA CGHAZ (in Fig. 1): Toughness of a multi-phase material showing brittle fracture is often controlled by the most brittle phase (in a manner of the weakest-link type failure), whereas its strength is typically governed by the rule-of-mixture of the hardness of constitutive phases. Thus, the M–A constituents are the phase contributing to both low toughness and high overall hardness.

Next, the role of hydrogen embrittlement in the LBZ phenomenon can be understood in terms of various crystalline defects in the CGHAZs. In steel, excessive hydrogen is possibly trapped by mechanical flaws (like cracks) and microstructural heterogeneities [14–16]. Some crystalline defects have lower activation energy for detrapping (or lower hydrogen-trap

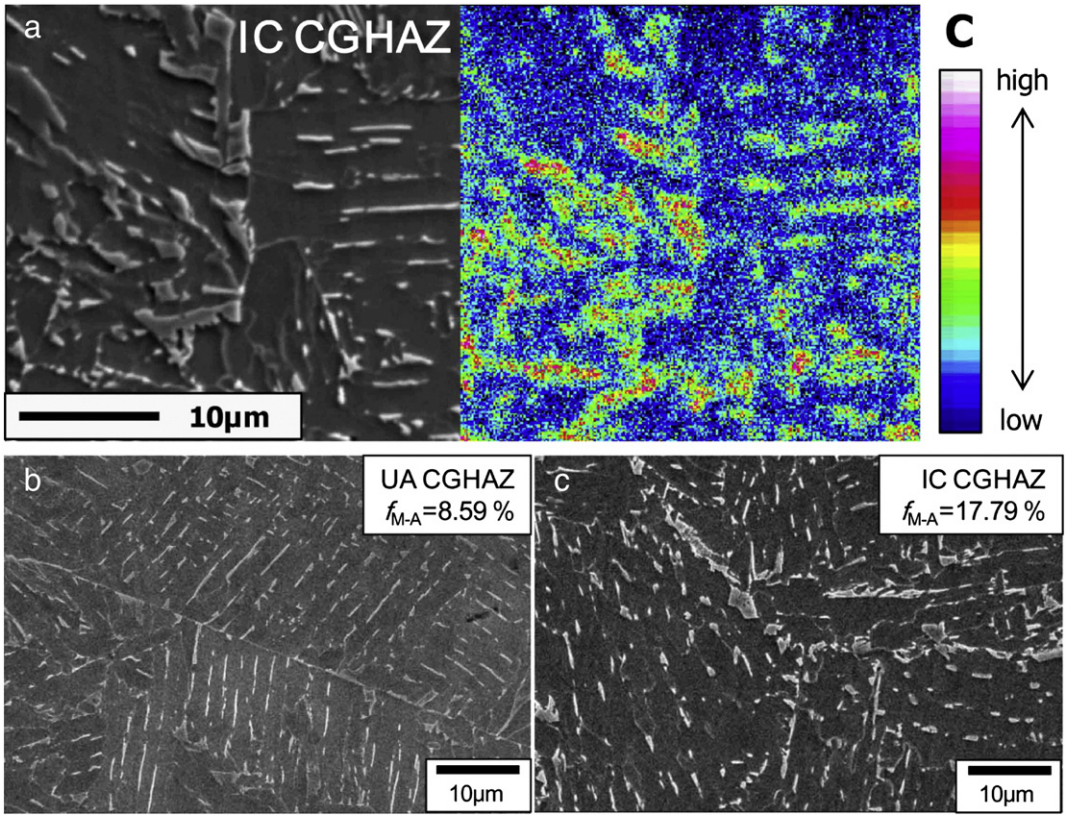

Fig. 4 – Observation of M–A constituents: (a) EPMA map; SEM images of (b) UA CGHAZ and (c) IC CGHAZ.

binding energy) than others; the activation energy becomes higher in the order of grain boundaries, dislocations, and microvoids (e.g., ~17, ~25, and ~36 kJ/mol, respectively, in Ref. [17]). The low binding energy traps (such as grain boundaries and dislocations) are known to be the main sources for hydrogen embrittlement and accelerate fracture by various mechanisms [18–20]; for example, when local concentration of hydrogen in trap sites exceeds some critical value, trapped hydrogen atoms decrease in cohesive strength of boundaries [21] or recombine into hydrogen molecule gas (and then the internal pressure developed by the gas can initiate the crack) [22]. Therefore, it has been argued that the trap sites for diffusive hydrogen can be more essential factor of hydrogen embrittlement than hydrogen itself and thus, increasing the potential trap sites can enhance the embrittlement of the steels [16,21]. Hydrogen effects in the present study can be also explained in a similar way. Hydrogen-induced toughness decrease in the SCR CGHAZ must be attributed to a large fraction of grain boundaries in its fine microstructure. In the IC and UA CGHAZ, high-density dislocations in the bainite structures may be the main hydrogen trap sites leading to the toughness decrease, and lath boundaries [23], M–A constituents [24], and interface between matrix and M–A constituents [25] can also act as additional trap sites.

As mentioned earlier, an interesting feature found in Fig. 3 is the presence of "splitting" in the H-charged IC and UA CGHAZ, which may play an important role in decreasing the toughness down to the absolutely low values. Although detailed mechanism of the splitting has not been fully understood yet, it was thought to be related with specific microstructural conditions including texture, inclusions such as MnS, anisotropic microstructures, band structures, elongated grain shape, segregation of P and S, and strip microstructure [26,27]. Among them, the elongated lath structure of the IC and UA CGHAZ can be the most likely source for the splitting observed here. However, because the splitting was not observed in the H-free samples, the role of the elongated structure should be understood together with the hydrogen effect. The hydrogen atoms trapped in specific sites (such as elongated lath boundaries and the interface between the lath and M–A constituents) can enhance decohesion of the boundaries and can easily initiate the cracks, which may accelerate splitting behavior.

4. Conclusion

Hydrogen effects on the toughness of the simulated CGHAZs in API X70 steel were investigated in search of the possible LBZs in hydrogen pipeline welds. After hydrogen charging, the IC and UA CGHAZ exhibited very low impact energy with the occurrence of splitting. The results are discussed in terms of combined effects of brittle microstructures and hydrogen trapping.

Acknowledgment

This work was supported by the Korea Research Council of Fundamental Science and Technology (KRCF) through the National Agenda Project, and partly by the Human Resources Development of the Korea Institute of Energy

Technology Evaluation and Planning (KETEP) grant funded by the Korea Government Ministry of Knowledge Economy (No. 20114010203020).

REFERENCES

[1] Gao M, Krishnamurthy R. Hydrogen fuel: production, transport, and storage [chapter 10]. In: Gupta RB, editor. New York: CRC Press; 2009.
[2] U.S. Department of Energy. Hydrogen, fuel cells and infrastructure technologies program multi-year research, development and demonstration plan, section 3.2, hydrogen delivery; January 21 2005.
[3] Oriani RA. Ann Rev Mater Sci 1978;8:327–57.
[4] López HF, Raghunath R, Albarran JL, Martinez L. Metall Mater Trans A 1996;27:3601–11.
[5] Wang R. Corros Sci 2009;51:2803–10.
[6] Kim BC, Lee S, Kim NJ, Lee DY. Metall Trans A 1991;22:139–49.
[7] Davis CL, King JE. Metall Mater Trans A 1994;25:563–73.
[8] Jang JI, Ju JB, Lee BW, Kwon D, Kim WS. Mat Sci Eng A 2003;340:68–79.
[9] Ju JB, Kim WS, Jang JI. Mater Sci Eng A 2012;546:258–62.
[10] Masubuchi K. Analysis of welded structures (chapter 2). New York: Pergamon Press; 1980.
[11] Andrews KW. J Iron Steel Inst 1965;203:721–7.
[12] American Petroleum Institute. Washington DC: API Specification 5 L; 2000.
[13] Ikawa H, Oshige H, Tanoue T. Trans Jpn Weld Soc 1980;11:3–12.
[14] Nagumo M. ISIJ Int 2001;41:590–8.
[15] Geng WT, Freeman AJ, Olson GB, Tateyama Y, Ohno T. Mater Trans 2005;46:756–60.
[16] Kim SM, Chun YS, Won SY, Kim YH, Lee CS. Metall Mater Trans A 2013;44:1331–9.
[17] Choo WY, Lee JY. Metall Trans A 1982;13:135–40.
[18] Chun YS, Kim JS, Park KT, Lee YK, Lee CS. Mater Sci Eng A 2012;533:87–95.
[19] Nagumo M, Takai K, Okuda N. J Alloy Comp 1999;293:310–6.
[20] Wei FG, Tsuzaki K. Metall Mater Trans A 2006;37:331–53.
[21] Nagumo M, Nakamura M, Takai K. Metall Mater Trans A 2001;32:339–47.
[22] Al-Mansour M, Alfantazi AM, El-boujdaini M. Mater Des 2009;30:4088–94.
[23] Gu JL, Chang KD, Fang HS, Bai BZ. ISIJ Int 2002;42:1560–4.
[24] Park GT, Koh SU, Jung HG, Kim KY. Corros Sci 2008;50:1865–71.
[25] Ren AX, Chu W, Li J, Su Y, Qiao L. Mater Chem Phys 2008;107:231–5.
[26] Shin SY, Hong S, Bae JH, Kim K, Lee S. Metall Mater Trans A 2009;40:2333–49.
[27] Yan W, Sha W, Zhi L, Wang W, Shan YY, Yang K. Metall Mater Trans A 2010;41:159–71.